

Probabilistic mapping of the antidystonic effect of pallidal neurostimulation: a multicentre imaging study

Martin M. Reich,^{1,2,*} Andreas Horn,^{3,*} Florian Lange,¹ Jonas Roothans,¹ Steffen Paschen,⁴ Joachim Runge,⁵ Fritz Wodarg,⁶ Nicolo G. Pozzi,¹ Karsten Witt,^{4,7} Robert C. Nickl,⁸ Louis Soussand,² Siobhan Ewert,³ Virginia Maltese,¹ Matthias Wittstock,⁹ Gerd-Helge Schneider,³ Volker Coenen,¹⁰ Philipp Mahlknecht,¹¹ Werner Poewe,¹¹ Wilhelm Eisner,¹² Ann-Kristin Helmers,¹³ Cordula Matthies,⁸ Volker Sturm,⁸ Ioannis U. Isaias,¹ Joachim K. Krauss,⁵ Andrea A. Kühn,³ Günther Deuschl⁴ and Jens Volkmann¹

*These authors contributed equally to this work.

Deep brain stimulation of the internal globus pallidus is a highly effective and established therapy for primary generalized and cervical dystonia, but therapeutic success is compromised by a non-responder rate of up to 25%, even in carefully-selected groups. Variability in electrode placement and inappropriate stimulation settings may account for a large proportion of this outcome variability. Here, we present probabilistic mapping data on a large cohort of patients collected from several European centres to resolve the optimal stimulation volume within the pallidal region. A total of 105 dystonia patients with pallidal deep brain stimulation were enrolled and 87 datasets (43 with cervical dystonia and 44 with generalized dystonia) were included into the subsequent ‘normative brain’ analysis. The average improvement of dystonia motor score was $50.5 \pm 30.9\%$ in cervical and $58.2 \pm 48.8\%$ in generalized dystonia, while 19.5% of patients did not respond to treatment (<25% benefit). We defined probabilistic maps of anti-dystonic effects by aggregating individual electrode locations and volumes of tissue activated (VTA) in normative atlas space and ranking voxel-wise for outcome distribution. We found a significant relation between motor outcome and the stimulation volume, but not the electrode location *per se*. The highest probability of stimulation induced motor benefit was found in a small volume covering the ventroposterior globus pallidus internus and adjacent subpallidal white matter. We then used the aggregated VTA-based outcome maps to rate patient individual VTAs and trained a linear regression model to predict individual outcomes. The prediction model showed robustness between the predicted and observed clinical improvement, with an r^2 of 0.294 ($P < 0.0001$). The predictions deviated on average by $16.9 \pm 11.6\%$ from observed dystonia improvements. For example, if a patient improved by 65%, the model would predict an improvement between 49% and 81%. Results were validated in an independent cohort of 10 dystonia patients, where prediction and observed benefit had a correlation of $r^2 = 0.52$ ($P = 0.02$) and a mean prediction error of 10.3% (± 8.9). These results emphasize the potential of probabilistic outcome brain mapping in refining the optimal therapeutic volume for pallidal neurostimulation and advancing computer-assisted planning and programming of deep brain stimulation.

- 1 Julius-Maximilians-University Würzburg, Department of Neurology, Germany
- 2 Beth Israel Deaconess Medical Center, Department of Neurology, Harvard Medical School, Boston, MA, USA
- 3 Charite-Universitätsmedizin Berlin, Movement Disorders and Neuromodulation Unit, Department of Neurology, Germany
- 4 University Kiel, Department of Neurology, Germany
- 5 MHH Hannover, Department of Neurosurgery, Germany
- 6 University Kiel, Department of Radiology, Germany
- 7 University Oldenburg, Department of Neurology, Germany

Received October 1, 2018. Revised December 12, 2018. Accepted January 8, 2019

© The Author(s) (2019). Published by Oxford University Press on behalf of the Guarantors of Brain. All rights reserved.

For Permissions, please email: journals.permissions@oup.com

- 8 Julius-Maximilians-University, Department of Neurosurgery, Germany
 9 University Rostock, Department of Neurology, Germany
 10 Freiburg University Medical Center, Department of Stereotactic and Functional Neurosurgery, Germany
 11 Department of Neurology, Innsbruck Medical University, Austria
 12 Department of Neurosurgery, Innsbruck Medical University, Austria
 13 University Kiel, Department of Neurosurgery, Germany

Correspondence to: Prof. Dr. med. Jens Volkmann
 University Hospital Wuerzburg
 Department of Neurology
 Josef-Schneider-Str.11
 D-97080 Wuerzburg
 Germany
 E-mail: Volkmann_J@ukw.de

Keywords: dystonia; deep brain stimulation; sweet spot; pallidal neurostimulation

Abbreviations: BFMDRS = Burke-Fahn-Marsden Dystonia Rating Scale; DBS = deep brain stimulation; GPe/i = external/internal globus pallidus; MNI = Montreal Neurological Institute; TWSTRS = Toronto Western Spasmodic Torticollis Rating Scale; VTA = volume of tissue activated

Introduction

Deep brain stimulation (DBS) of the internal globus pallidus (GPi) is an established therapy for primary generalized and cervical dystonia (Vidailhet *et al.*, 2005, 2007; Volkmann *et al.*, 2012, 2014). The average improvement of dystonia severity in patients with primary dystonia amounts to 50–60% in most clinical studies, depending on the timing of assessment, the type of dystonia, and the rating scale used (Isaias *et al.*, 2008; Volkmann *et al.*, 2012, 2014; Bruggemann *et al.*, 2015; Contarino *et al.*, 2016). However, outcomes are often variable and randomized controlled trials report up to 25% of non-responders (defined as <25% score improvement), even in carefully selected groups of primary dystonia patients (Volkmann *et al.*, 2012). Variability in electrode placement and inappropriate stimulation settings may account for a large proportion of outcome variability (Pauls *et al.*, 2017), but patient selection criteria—including uncertainties in the clinical classification of the dystonia—must not be underestimated.

The variability of the globus pallidus position in the anterior–posterior commissure (AC-PC)-based coordinate space and low magnetic resonance contrast of the nucleus are challenges in reliably delineating the stereotactic target for pallidal DBS (Vasques *et al.*, 2009). Moreover, the delayed improvement of dystonic symptoms following DBS initiation complicates the selection and titration of stimulation parameters based on clinical response testing (Kupsch *et al.*, 2011). Both problems may result in inappropriate stimulation volumes and suboptimal therapy outcomes. Hence, there is a need for defining the ‘optimal efficacy volume’ within the pallidal area (Contarino *et al.*, 2016), which could then be used to guide electrode implantation and post-operative programming. Previous studies have focused on identifying active contact locations or mean electrical charge distributions of effective stimulation

in single-centre patient cohorts. Limitations of these studies include the small sample size and limited spatial coverage of the pallidal target region due to relatively invariant electrode placements of single neurosurgeons. Nevertheless, they have indicated good outcomes related to an electrode location within the ventral and posterior aspect of internal globus pallidus (Tisch *et al.*, 2007; Hamani *et al.*, 2008; Cheung *et al.*, 2014; Park *et al.*, 2017). Here, we present probabilistic mapping data on a large cohort of patients collected from several European centres to resolve the optimal stimulation volume within the pallidal region.

Materials and methods

Subjects

This study retrospectively enrolled datasets of 105 subjects with dystonia treated chronically with bilateral pallidal DBS and operated at seven different European DBS centres. Screening criteria were the diagnosis of isolated generalized and segmental dystonia or cervical dystonia according to the Consensus Statement of the Movement Disorder Society Group (Albanese *et al.*, 2013) and chronic pallidal DBS therapy. Sixteen of 105 patients took part in a sham-controlled trial of DBS for cervical dystonia (Volkmann *et al.*, 2014) and 22 of 105 patients in the randomized trial of DBS for primary generalized and segmental dystonia (Kupsch *et al.*, 2006; Volkmann *et al.*, 2012). Individual datasets were included into this study if they contained: (i) a video recording depicting their motor state within 6 months before surgery and a second assessment at long-term follow-up (at least 12 months for cervical and 36 months for generalized or segmental dystonia); (ii) pre- and post-operative neuroimaging allowing reconstruction of lead location; and (iii) preoperative brain MRI without any signs of structural brain damage. Exclusion criteria were a diagnosis of combined (or complex) dystonia or prior ablative surgery. An additional group of 10 patients with isolated dystonia treated with bilateral pallidal

neurostimulation at the University Hospital of Würzburg or Charité-Universitätsmedizin Berlin was recruited for validation purposes. This cohort had a slightly shorter follow-up (at least 9 months for cervical and 12 months for generalized or segmental dystonia) and was implanted with another neurostimulation system capable of constant current stimulation (Vercise RC, Boston Scientific Inc.). The study was carried out in accordance with the Declaration of Helsinki and approved by the institutional review board of the University Hospital of Würzburg (registration no. 150/15).

Surgical procedure and clinical evaluation

The surgical procedure was similar in all centres, and has been described previously (Volkman *et al.*, 2014). All patients received quadripolar macroelectrodes (model 3389 or 3387, Medtronic Inc.) or an octopolar macroelectrode (model 2201-A, Boston Scientific Inc.) into the postero-ventral GPi. The neurostimulation parameters were programmed according to best clinical practice by the local DBS neurologist, based on clinical response testing (Kupsch *et al.*, 2011). We collected pre- and post-operative video sequences of all patients. All video sequences were rated retrospectively by the same movement disorder neurologist (M.M.R.), using either the Toronto Western Spasmodic Torticollis Rating Scale (TWSTRS) in subjects with cervical dystonia or the Burke-Fahn-Marsden Dystonia Rating Scale (BFMDRS) in patients with generalized or segmental dystonia. Results were normalized by calculating the percentage change of the TWSTRS and the BFMDRS.

Deep brain stimulation lead localization and volume of tissue activated modelling

Visualization of the electrode position was established using SureTune™ software (Medtronic Eindhoven Design Center, MEDC) by fusing the individual preoperative MRI used for stereotactic planning with post-operative CT or MRI depicting the lead location. To visualize the electrode locations, the leads were identified by the CT or MRI artefact, as described previously (Pollo *et al.*, 2004; Hemm *et al.*, 2009) and represented in the Yelnik atlas (Yelnik *et al.*, 2007). The atlas was registered onto regions of interest on the GPi, external globus pallidus (GPe) and striatum using a rigid semi-automatic registration algorithm on T₂-weighted fast spin echo MRI and/or T₁-weighted inversion recovery pulse MRI sequences for each patient. This was done for the left and right hemisphere separately. The volume of tissue activated (VTA) was computed for each lead based on the applied stimulation parameters (Table 1) using an algorithm previously described by Astrom *et al.* (2015). Images were then linearly normalized into Montreal Neurological Institute (MNI; ICBM 2009b NLIN asymmetric) space, based on the local atlas registrations using a self-programmed MATLAB tool, thereby projecting all data onto the left hemisphere. Of note, after registering the VTAs to the local pallidal atlas, the same transform was applied to each to register them into MNI space.

Anatomical-clinical correlations

All electrodes and related VTAs were associated with the corresponding motor improvement score (percentage change). In subjects with cervical dystonia, the TWSTRS motor score improvement without using the duration factor (item Ib) was assigned to both hemispheres equally; this modified motor score was chosen because the total TWSTRS motor score is too strongly weighted by the duration factor with respect to the improvement of dystonic postures (Volkman *et al.*, 2014). In subjects with generalized or segmental dystonia, the global improvement in BFMDRS was associated with the stimulation of both hemispheres (see Fig. 1 for overview of the methods and Fig. 2 for variability in outcome).

Creation of electrode-outcome maps

The four contacts on each lead were categorized as active or inactive. For the active contacts, four groups based on the improvement of dystonia motor scores were possible: no response (<25%), poor response (25–50%), good response (50–80%), excellent response (>80%). After transferring the electrode locations to the common anatomical reference space, outcome maps were created by displaying all electrodes and colour-coding them based on the associated clinical benefit. If more than one cathode was active, the point directly between both contacts was taken. Additionally, the electrodes were classified based on their anatomical location in the Yelnik atlas: within the GPi, GPe, or white matter (see Fig. 3 for an overview). A Barnard's exact test (Trujillo-Ortiz *et al.*, 2004) was run in MATLAB to test for significant differences in contact selection and/or clinical response by anatomical location.

Creation of volume of tissue activated-based outcome maps

After registering all VTAs into the common anatomical reference space (ICBM 2009b NLIN asymmetric), every voxel (0.25 × 0.25 × 0.25 mm) in that space was covered by either none, a single, or multiple VTAs. Consequently, a voxel could be associated with a multitude of dystonia score changes depending on the density of VTAs. To evaluate if the motor outcomes associated with a given voxel were significantly different from all other dystonia score changes not associated with stimulation of this particular voxel, a two-sample *t*-test was performed. This test returns *t*-statistic and *P*-values for every voxel that can be displayed as 3D statistical maps. After applying a cluster threshold of >500 voxels, significant clusters (uncorrected *P* < 0.05) were visualized as volumes of high or low likelihood of good outcome (sweet spots). 'Good' and 'poor' outcome clusters were distinguished based on the sign of the *t*-statistic. Results were reported for generalized (or segmental) and cervical dystonia patients separately. If both sweet spots shared the same location, the groups were combined to increase spatial resolution using an uncorrected *P*-value threshold of <0.01 (cluster threshold of >500 voxels).

Table 1 Demographic and clinical patient characteristics

Characteristic	Cervical dystonia			Generalized dystonia		
	Total	Image analysis subset	P	Total	Image analysis subset	P
Number of patients	53	43		52	44	
Age at surgery, years	56.3 (10.5)	57 (16.3)	0.80	39.8 (16.7)	47.8 (16.3)	0.02
Disease duration prior to surgery, years	10.6 (7.4)	11.1 (7.8)	0.75	18.0 (10.7)	18.1 (10.7)	0.96
Age of disease onset	45.3 (11.1)	45.9 (11.4)	0.80	21.4 (18.6)	22.9 (19.0)	0.70
<i>DYT1</i> testing positive	-	-	-	12 of 34	8 of 29	0.59*
Dystonia severity (TWSTRS/BFMDRS) at baseline	20.5 (3.7)	20.5 (3.6)	1	45.0 (25.3)	45.2 (26.1)	0.97
Follow up time, months	14.8 (7.6)	15.0 (7.6)	0.90	44.1 (15.3)	43.6 (15.9)	0.88
Dystonia severity (TWSTRS/BFMDRS) at follow-up	10.3 (6.6)	10.1(6.5)	0.88	16.7 (17.9)	16.3 (17.1)	0.91
Improvement in dystonia motor score, %	49.1 (32.6)	50.5 (30.9)	0.83	59.5 (46.3)	58.2 (48.8)	0.89
<i>n</i> (%) of non-responders, <25% improvement	11 (20.1)	9 (20.9)	1*	9 (17.3)	8 (18.2)	1*
Stimulation parameters						
Amplitude, voltage/impedance, mA	3.5 (1.3)	3.5 (1.4)	1	3.6 (1.6)	3.5 (1.2)	0.74
Pulse width, μ s	115.5 (51.0)	108.8 (48.9)	0.52	119.4 (37.2)	115.2 (34.0)	0.57
Frequency, Hz	149.9 (29.8)	151.3 (30.9)	0.82	150.3 (27.0)	149.9 (26.9)	0.94

Data are presented as mean (SD), unless otherwise stated. *P*-values follow from two sample student *t*-tests, *except for binomial distributions where a Fisher test was performed.

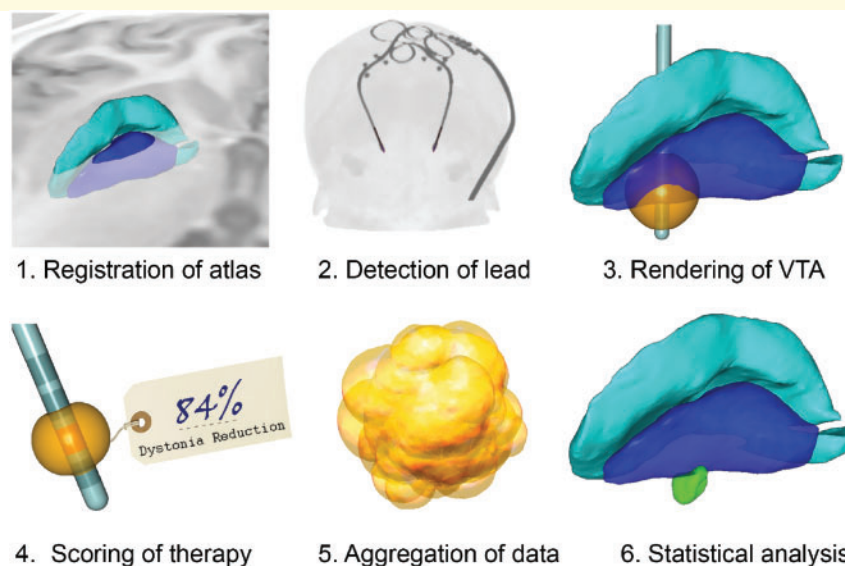


Figure 1 Workflow of sweet spot analysis. The image analysis workflow that yields the sweet spot is summarized in six consecutive steps. Steps 1–3 are performed using SureTune software. Both the registration of the atlas and detection of lead were performed semi-automatically and were manually validated. Then the data was exported to MATLAB, where steps 4–6 were done with custom built scripts. The volumes of tissue activated (VTAs) were labelled with clinical scores (4) and brought together to a common space (ICBM 2009b NLIN) based on the registered atlases (5). Finally, a statistical analysis for each voxel resulted in a heat map, from which a sweet spot (green) could be distilled.

Validation of image co-registration and normalization procedure

In a subset of 15 subjects operated at Charité, Berlin, we applied an alternative method of lead localization and normalization as described by Horn and Kühn (2015). Briefly, post-operative MRI were linearly co-registered to preoperative MRI using SPM12 (<http://www.fil.ion.ucl.ac.uk/spm/software/spm12/>). Images were then normalized into the ICBM 2009b NLIN asymmetric space using the SyN approach

implemented in advanced normalization tools (<http://stnava.github.io/ANTs/>), based on the preoperative MRI. DBS electrode contacts were localized within the MNI space and VTAs were simulated using Lead-DBS software (Horn *et al.*, 2017). The subsequent reconstruction of VTA-based outcome maps followed the same method as described above. To test the similarity of the heat maps (*t*-maps) obtained by either the SureTune or Lead-DBS, we performed a spatial correlation analysis calculating Spearman and Pearson's linear correlation coefficient.

Statistical analysis and outcome prediction models

Multivariate regression analysis was used to analyse the effect of demographic (age at onset, age at surgery and disease duration) and clinical quantitative variables (total scores for the movement and disability scales) on the therapeutic outcome (percentage change of the TWSTRS and the BFMDRS). The same analysis was performed for electrical stimulation settings

(current and charge delivery). We used a Wilcoxon test for categorical variables [gender and *TOR1A* (*DYT1*) status]. Statistical tests were two-tailed and $P < 0.05$ was considered statistically significant.

Two methods were examined to predict therapeutic outcome based solely on active contact locations. A relatively simple method was used to predict the improvement of each lead, based on a weighted average of improvement scores for its surrounding active contacts. The weights were inversely proportional to the distance to make nearby electrodes weigh stronger than electrodes far away. A more elaborate method was used to explore the space on a 0.1 mm grid, to find the optimal location that predicted the outcome. The location to which the distances showed the highest positive and highest negative correlations with respect to the improvement were used as a covariate. For both active-contact location-based methods, a linear regression was performed.

Subsequently, we analysed the correlation between the VTA and the individual improvement. VTAs model the hypothetical volume of action potential initiation by DBS and depend on both, the electrode location and stimulation settings. Left and right VTAs were combined, reflecting the bilateral treatment of patients. We created a prediction model for scores of individual VTAs based on their placement within the VTA atlas. In detail, the voxel wise analysis compares the distribution of improvement scores of the entire population assigned to a single voxel in atlas space to all improvement scores not included in that voxel. The two resulting outcome distributions are then compared by means of a Student's *t*-test with the null hypothesis of equality. The sign of the *t*-statistic (*T*-map) indicates if the tested voxel has higher or lower improvement scores than the mean. The *P*-value or corresponding *P*-statistic (*P*-map) provides a measure how strongly the outcome distribution of a voxel deviates from the average but it does not

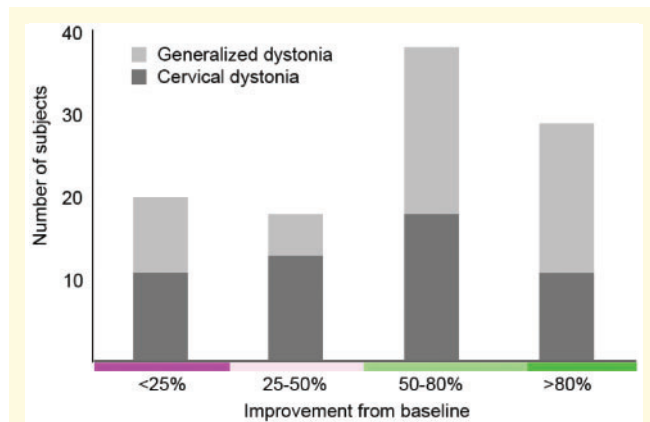


Figure 2 Variability in response of dystonic symptoms to pallidal deep brain stimulation. Improvement indicated on the TWSTRS for cervical or BFMDRS for generalized dystonia compared to baseline. Each patient was grouped into one of the four response categories: non-responder (<25%; purple), average responder (25–50%; pink), good responder (50–80%; light green) and super-responder (>80%; dark green).

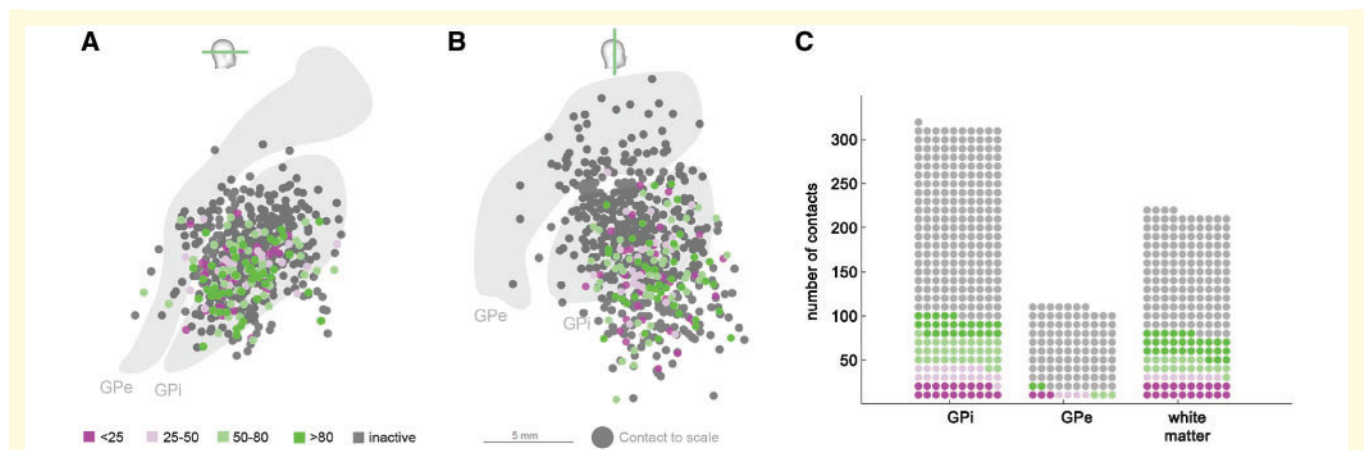


Figure 3 Anatomical distribution of all implanted electrodes. The anatomical location of all electrodes of 174 leads is depicted on the Yelnik Atlas (Yelnik *et al.*, 2007). Inactive contacts are in grey, active contacts are colour-coded, based on stimulation-induced motor score improvement. In horizontal (A) and frontal (B) view contact size is scaled down by 75% with respect to the pallidum for a better overview. The total of 696 electrodes of 174 leads in 87 subjects were classified according to their atlas-based location inside the GPI, GPe or subpallidal white matter (C). A grey colour denotes inactive electrodes. The percentage of motor score improvement associated with an electrode is colour-coded purple (<25%), pink (25–50%), light green (50–80%) and dark green (>80%). Most electrodes were located inside the GPI and subpallidal white matter. Among all available electrode contacts, a significantly larger proportion of activated contacts were located in subpallidal white matter compared to those located inside the GPI ($P < 0.001$).

contain information about the side of the distribution (above or below average). Therefore, the T -map and the P -map are combined into a so called heat map (or signed- P map). The population heat map is used to evaluate and rate patient specific VTAs. We calculate the spatial overlap between the patient-specific VTA and the heat map, which results in a distribution of heat map values for included voxels. This distribution is fed into a linear model and used for training. The trained parameters can then be applied to any new distribution and an individual improvement score will be calculated. This analysis was run on data from both datasets (cervical and generalized or segmental dystonia) combined, and results were correlated with measured clinical outcome. All analyses were performed in a leave-one-out fashion (see below). Additionally, we validated our model by training only on cervical dystonia patients and showing their association with motor improvement in patients with generalized dystonia. This analysis was also done using the generalized dystonia data to train and forecast the outcome in cervical dystonia patients.

Finally, we validated the predictive value of these VTA-atlas model estimations. A statistic and rigorous method to do so is a leave-one-out cross-validation (Arlot and Celisse, 2010). Here, the model is trained using $n - 1$ subjects and validated on the left out subject, iterating n times to complete the full cohort. In other words, for each subject as described an outcome distribution was computed, and a novel VTA-atlas model was computed based on the remaining subjects. Of relevance, this time the multivariate linear regression models were also conducted in a leave-one-out-manner, thus creating an independent prediction model for each subject. Based on these model predictions, the mean prediction error was calculated by plotting against the measured clinical outcome and three patients were selected as representative examples. Furthermore, we validated the predictive value of these VTA-atlas model estimations also in an independent cohort of dystonia subjects implanted with a multiple-independent current source neurostimulator. Here, the model trained by the combined dataset (cervical and generalized or segmental dystonia) and outcome of the independent cohort were predicted by applying both VTAs of a subject. Prediction values of the VTA-atlas model of all subjects were then associated with the clinically observed outcome in a linear regression model. Additionally, mean prediction error was calculated.

Ultimately, to illustrate the potential of this method for computer-assisted programming of DBS we exhaustively evaluated a predefined VTA (3.0 mA; 90 μ s) in all possible contact positions of each patient. All 16 monopolar electrode combinations of each patient were tested in the VTA-atlas model and the best *in silico* setting (i.e. highest degree on dystonia improvement) was determined for comparison with the clinically derived programming choices. For all patients included in the imaging analysis, we then calculated and compared the predicted outcome of the best *in silico* programming choice and the clinically defined program setting.

Statistical analyses were performed with the JMP statistical package, version 13 (SAS Institute, Inc., Cary, NC, USA) or with MATLAB Statistics and Machine Learning Toolbox (version 2017a, Mathworks). Results are presented as mean \pm standard deviation (SD).

Data availability

The data that support the findings of this study are available on request from the corresponding author. The data are not publicly available due to their containing information that could compromise the privacy of research participants.

Results

Clinical characteristics

A total of 105 dystonia patients with pallidal DBS were enrolled. Fifty-three subjects with cervical dystonia had a mean TWSTRS score reduction of $49.1 \pm 32.6\%$ at 14.8 ± 7.6 months after surgery. Fifty-two subjects with generalized or segmental dystonia improved by $59.5 \pm 46.3\%$ at 44.1 ± 15.3 months after surgery on the BFMDRS motor score (Table 1). The proportion of non-responders (<25% improvement) was 20.1% for the cervical dystonia group and 17.3% for the generalized and segmental dystonia group. An ‘excellent’ clinical response (motor score improvement >80%) was observed in 20.1% and 34.6% of patients, respectively (Fig. 2). No significant differences in relative improvement were noted between the dystonia groups ($P = 0.21$). The independent test cohort had a mean dystonia improvement of $63.1 \pm 20.0\%$ at 12.0 ± 2.4 months after surgery (details in [Supplementary Table 1](#)).

Among demographic and clinical variables, only disease duration significantly correlated with clinical outcome in this cohort of patients ($\rho = -0.39$, $P < 0.05$). A positive *DYT1* status (13 patients) was not associated with better motor improvement ($P > 0.84$). The two dystonia groups did not differ in stimulation parameters: the amplitude was 3.5 ± 1.3 mA in cervical dystonia and 3.6 ± 1.6 mA in generalized dystonia ($P = 0.44$), the frequency was 149.9 ± 29.8 Hz and 150.3 ± 27.0 Hz, respectively ($P = 0.33$), while the pulse width was 115.5 ± 51.0 μ s and 119.4 ± 37.2 μ s ($P = 0.93$). We did not find an association between charge injection (amplitude \times pulse width)—i.e. a larger VTA—and clinical improvement.

Aggregated analysis of electrode locations and volumes of tissue activated

First we localized electrodes in standard stereotactic reference space: individual AC-PC-based coordinates of the active electrodes in all 105 patients were: 19.8 ± 1.8 mm lateral, 3.9 ± 1.5 mm anterior and 1.2 ± 2.3 mm inferior to the midcommissural point in cervical dystonia, and 19.8 ± 1.7 mm lateral, 3.6 ± 1.6 mm anterior and 1.2 ± 2.4 mm inferior in generalized or segmental dystonia. These coordinates did not differ

between the two dystonia groups ($P_x = 0.98$, $P_y = 0.18$, $P_z = 0.61$).

A total of 87 of 105 datasets (i.e. a total of 174 leads or 696 contacts) were included into the subsequent, ‘normative brain’ analysis. Reasons for excluding datasets were: missing preoperative T_1 image with slice thickness ≤ 2 mm (12 subjects), low quality post-operative CT or MRI scan without slice thickness ≤ 2 mm (five subjects), and missing stimulation settings (one subject). For clinical characteristics of the entire patient cohort and the final image analysis subset, see Table 1.

After normalizing images into the MNI space [ICBM 2009b NLIN (Fonov *et al.*, 2009)], a wide variety of lead locations was observed in the pallidal region (Fig. 3). In the horizontal plane, the most active electrodes clustered within the posterior and lateral segment of the GPi. Less consistency was observed in the frontal plane, with electrodes spanning a distance of 13.2 mm along the z -axis. After classifying electrodes based on their atlas location, we found that among all available electrode contacts, mostly those selected for chronic stimulation were located inside GPi and white matter; a significantly larger proportion of activated contacts were located in subpallidal white matter compared to inside the GPi ($P < 0.001$) (Fig. 3). We also found a trend of active contacts in subpallidal white matter being associated with a larger proportion of good or excellent outcome (improvement $> 50\%$) compared to those inside the GPi ($P = 0.071$). However, the observed associations between electrode location and outcome were small, and the reconstructed electrode-outcome map (Fig. 3) did not reveal any clear topographical clusters of electrodes with ‘favourable’ or ‘poor’ therapeutic response. In fact, electrodes mediating excellent responses ($> 80\%$ improvement) or therapeutic failures ($< 25\%$ improvements) were tightly intermingled in normative atlas space.

A final analysis considered the stimulation parameters associated with each electrode by calculating the individual VTAs and transforming them into normative atlas space. The aggregated volume of all individual VTAs amounted to 2.3144 mm³ and covered almost the entire pallidal complex. The model-based analysis of 174 outcome-classified VTAs returned a 3D heat map depicting the anatomical distribution of the probability value of stimulation-induced outcome within this patient cohort (VTA-based probabilistic outcome map). Thresholding for the upper 95% or 99% confidence limit of the outcome distribution resulted in small contiguous clusters of voxels associated with significantly above average motor outcome, which we termed the antidystonic sweet spots. They were located within the ventroposterior GPi and adjacent subpallidal white matter, and showed complete overlap when reconstructed for the two dystonia groups separately or combined (Fig. 4). The centre of gravity of the sweet spot volume for the entire cohort was 19.4 mm lateral, 3.2 mm anterior and 1.9 mm inferior to the midcommissural point in AC-PC-based stereotactic reference space (MNI coordinates: $x = -19.4$ mm;

$y = -10.1$ mm; $z = -5.9$ mm). The validation analysis, using an observer-independent method of image co-registration and normalization (Lead-DBS), demonstrated a high spatial agreement of the reconstructed heat maps as reflected by a Spearman and Pearson correlation coefficients of $\rho = 0.63$ ($P < 0.001$) and $\rho = 0.62$ ($P < 0.001$), respectively.

Outcome prediction models

Active contact location was not significantly correlated with clinical improvement provided by pallidal DBS, based on the weighted average of improvement scores of its surrounding active contacts ($r^2 = 0.01$; $P = 0.17$). Using the more elaborate method of distance to the computed optimal location of contacts, the association with clinical improvement fell just short of our statistical threshold for correlations ($r^2 = 0.11$; $P = 0.06$). In contrast, we found strong correlations between clinical outcome and the individual stimulation volume within the probabilistic outcome atlas (VTA atlas): the outcome distributions produced from this VTA atlas were highly associated with observed clinical outcome ($r^2 = 0.534$; $P < 0.0001$). In other words, the VTA-atlas model estimations explained 53% of the variance of motor score improvement (Fig. 5). By adding clinical and demographic variables to the multivariate regression model (disease duration before surgery, age at surgery, age at onset and dystonia severity at baseline), we were able to explain 59.7% of the observed variance in DBS response. Likewise, the VTA-atlas model trained only on patients with cervical dystonia was predictive in the generalized cohort ($r^2 = 0.23$; $P < 0.0001$) and vice versa ($r^2 = 0.33$; $P < 0.0001$) (Supplementary Fig. 1).

Motivated by these findings, we analysed the predictive value of our VTA-atlas estimations for each individual outcome using the leave-one-out cross-validation. The underlying prediction model showed robustness between the predicted and observed clinical improvement, with an r^2 of 0.294 ($P < 0.0001$). The predictions deviated on average by $16.9 \pm 11.6\%$ from observed dystonia improvements. For example, if a patient improved by 65%, the model might have predicted an improvement between 49% and 81%. Including additional clinical variables (disease duration before surgery, age at surgery, age at onset and dystonia severity at baseline) only slightly increased the predictive value (mean error 15.3 ± 10.9). The VTA atlas-based predictions of three illustrative patients are shown in Fig. 6. Furthermore, we tested the VTA-atlas estimation on an independent cohort of 10 dystonia patients implanted in Berlin and Würzburg with another neurostimulation system (Vercise RC, Boston Scientific Inc.). Despite technical differences in delivering the neurostimulation (single source constant voltage versus multiple independent current source pulse generator), the VTA-atlas based model predicted the observed clinical improvements in

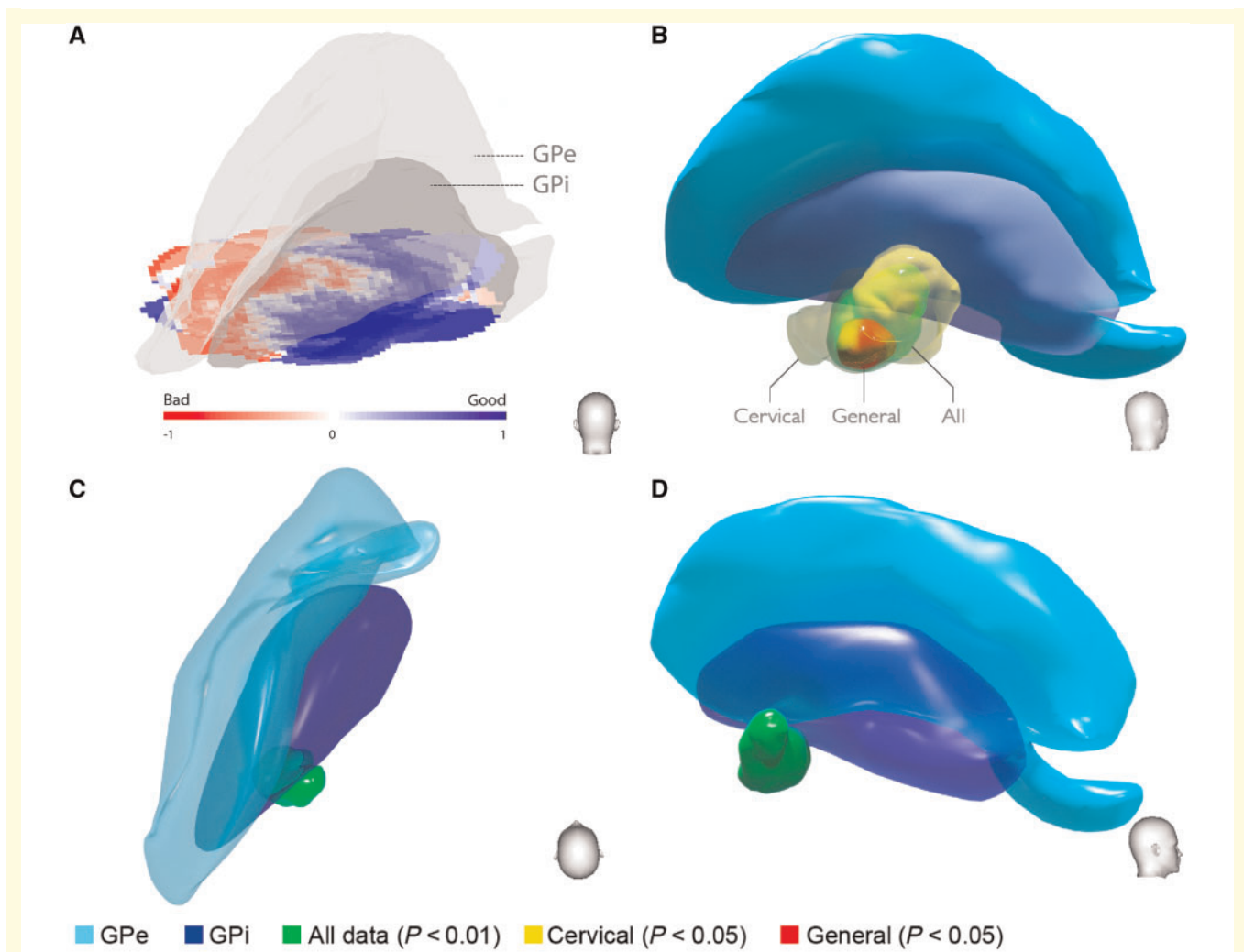


Figure 4 Outcome probability of pallidal neurostimulation for dystonia. The image shows the results of the voxel-wise statistical VTA analysis of 87 dystonia subjects with respect to the dystonia motor score reduction. **(A)** Heatmap of all dystonia subjects based on signed P -values (a combined t -statistic and P -value; see 'Materials and methods' section for details). **(B)** There was a similar anatomical position of voxels with highest probability of good outcome, with $P < 0.05$ in cervical (yellow) and generalized (red) and $P < 0.01$ in all subjects (green). The position of the 'anti-dystonic sweet spot' arrogated from 174 different VTAs with different clinical responses ($P < 0.01$; cluster size threshold > 500 voxels) is shown in the axial **(C)** and sagittal **(D)** view.

the validation cohort with a mean error of 10.3% (± 8.9) ($r^2 = 0.52$; $P = 0.02$) (Fig. 6D).

To illustrate the potential value of our model for computer-assisted programming of DBS, we simulated an exhaustive evaluation of a predefined VTA (3.0 mA; 90 μ s) in all possible monopolar electrode choices of each patient. This VTA-atlas based simulation predicted a mean improvement of 76.8 ± 15.3 % ($P < 0.03$) for the model based, 'optimal' programming settings in 87 dystonia patients as compared to the 60.5 ± 21.9 % observed with clinical programming choices (Fig. 7). More importantly, 54 leads in this group had a clinically observed improvement of $< 50\%$, but *in silico* testing of all possible electrode choices predicted only seven leads with an expected improvement $< 50\%$.

Discussion

Our study provides evidence that variable clinical outcomes of pallidal DBS for dystonia may to a relevant degree be explained by the exact location and extent of the stimulation volume within the pallidal region and adjacent white matter. Different electrode positions may create VTAs, which overlap in the most sensitive regions of GPi and adjacent white matter. This may explain the observed stronger association between stimulation volume and outcome, explaining 53% of the variance in our cohort, as compared to the electrode position alone. Our method of calculating a probabilistic outcome map from a large group of patients with known stimulation volumes and DBS outcomes, which is then used to estimate the

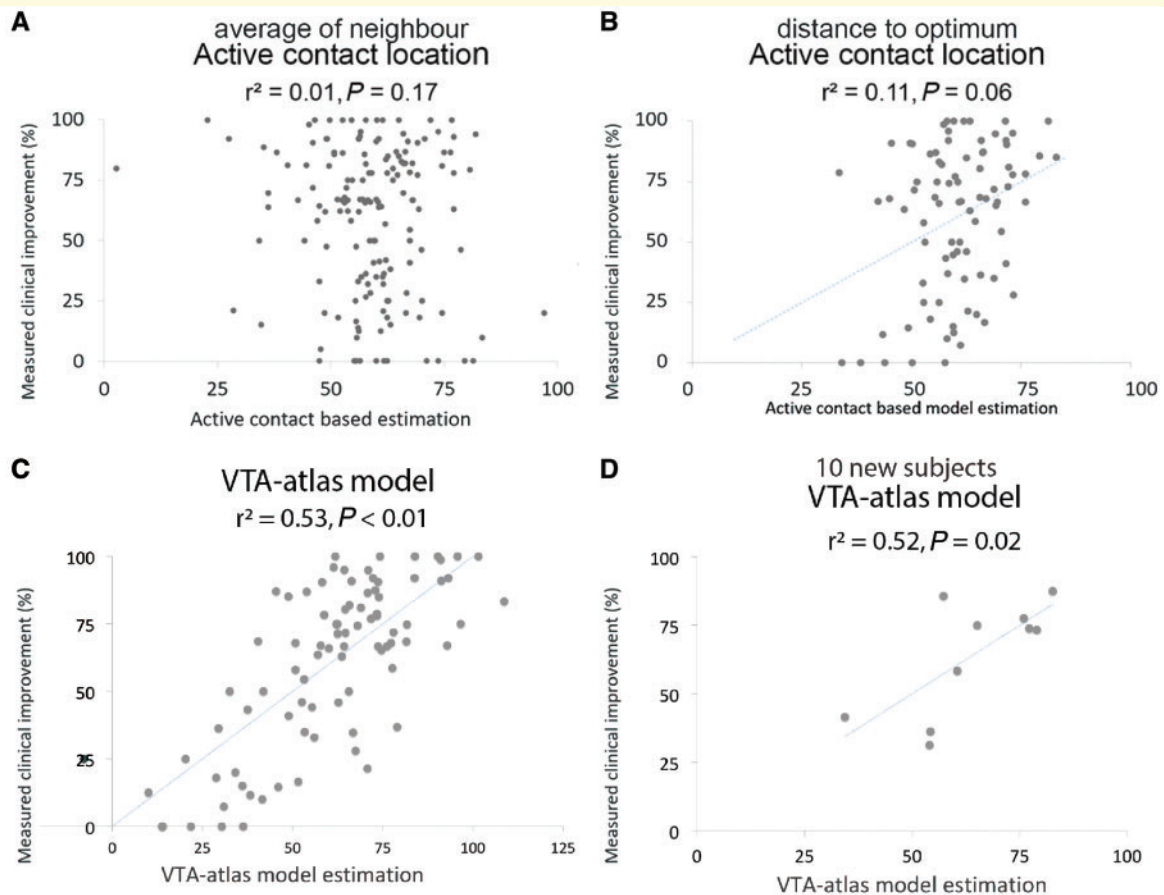


Figure 5 Correlation of observed clinical improvement with active contact location and VTA-atlas model estimation. The active contact location was not significantly correlated with clinical improvement provided by pallidal deep brain stimulation (A and B). In contrast, patients with higher scores in the VTA atlas estimation improved significantly more than patients with a low score (C). The atlas estimation used the spatial overlap between the patient specific VTA and the heat map, which results in a distribution of heat-map values for included voxels. This distribution is fed into a linear model and used for training. The trained parameters can then be applied to any new distribution and an individual improvement score will be calculated, which is done here for all patients in a leave-one-out fashion. (D) VTA-atlas-based prediction in an independent dataset of 10 patients with dystonia, forecasting the measured clinical improvement within a mean error of 10.3% (± 8.9).

expected benefit based on electrode positions and stimulation settings, could be an important advance towards computer-assisted planning and programming of DBS in dystonia.

Efficacy of pallidal deep brain stimulation

Deep brain stimulation of the GPi is among the most effective treatments for severe, isolated dystonias. However, most neurologists and patients still see DBS as a last-line therapy, and for the large group of adult-onset focal dystonias it is not an established alternative to botulinum toxin treatment. This is surprising, because DBS is relatively safe and targets the pathophysiology of dystonia, which is a classical basal ganglia circuit disorder. The main reason for some reluctance towards DBS may be the inconsistency

of outcomes even in experienced centres. Clinical trials have reported a non-responder rate of up to 25% (Kupsch *et al.*, 2006; Volkmann *et al.*, 2012; Walsh *et al.*, 2013). More alarmingly, it has not been possible to identify clear causes for these treatment failures, which might be modified by better guidelines for patient selection, surgical performance or post-operative management. Some patient-related factors have been identified as weak modifiers of outcome, such as short(er) disease duration and genetic status (Isaias *et al.*, 2008; Andrews *et al.*, 2010; Jinnah *et al.*, 2017). Hence, uncertainty is associated with every DBS procedure in dystonia and contrasts unfavourably with the high expectations of each surgical candidate.

Our cohort of 105 dystonia patients operated at seven European academic centres is representative for the current clinical standard of pallidal DBS in isolated dystonia in terms of patient characteristics and outcomes. Group

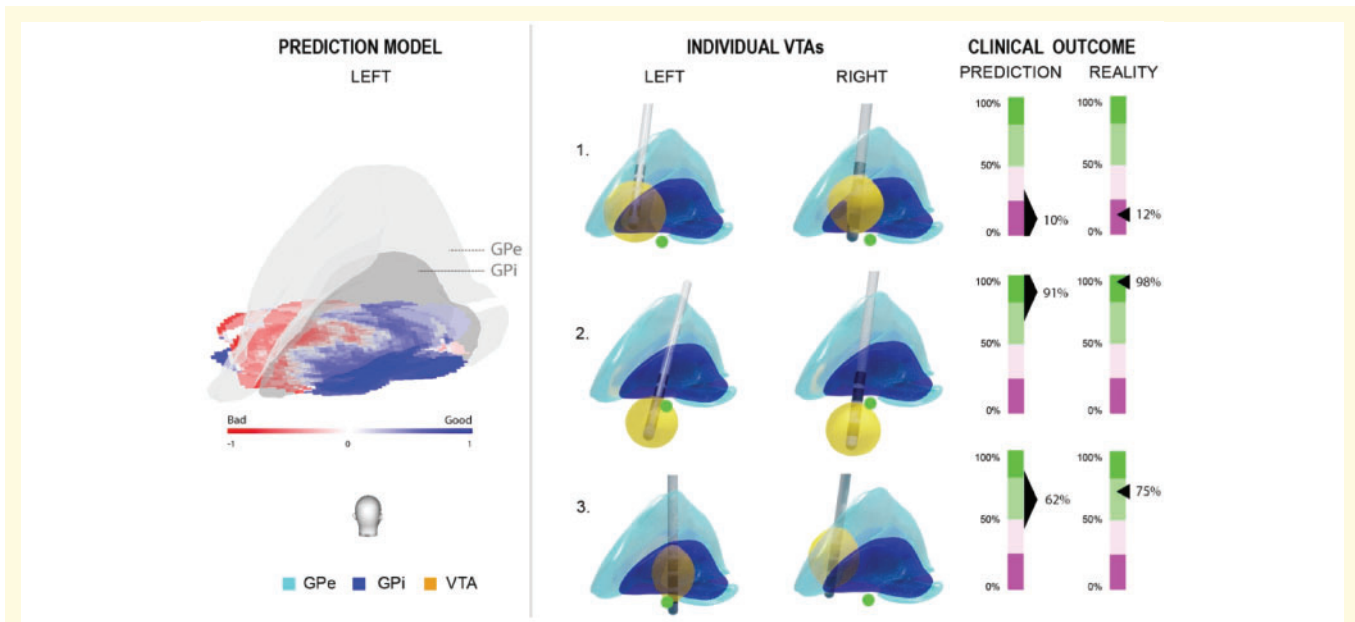


Figure 6 VTA-atlas prediction modelling in three dystonia patients with pallidal DBS. The image shows the clinical outcome prediction in individual patients based on the VTA atlas of their stimulation. The current algorithm uses the prediction model, spatial overlap between the patient specific VTA and the heat map, which results in a distribution of heat map values for included voxels. Clinical response was predicted based on this distribution within a mean error of $15.6 \pm 12.5\%$. Selected examples include a non- and a super-responder with accurate prediction (*top* and *middle*), and a good responder (*bottom*). Interestingly, none of the individual VTAs covered the spot of highest outcome probability (green area, with a $P < 0.05$), but the prediction model on the whole VTA-atlas map was able to provide an accurate prediction. This illustrates the limitation of a statistical group finding (e.g. the sweet spot) on an individual level. In other words, a stimulation of the sweet spot is not necessary for an individual good motor outcome, but the statistical likelihood is higher. Green dots in the middle column indicate the position of the spot of highest outcome probability in the individual anatomical space of these subjects.

mean motor score improvements and their distribution were consistent with the literature (Holloway *et al.*, 2006). In fact, large variance in the clinical outcome data as well as in lead positions was essential for our probabilistic analysis approach.

Antidystonic sweet spot location and pathophysiological implications

Pallidal DBS is a complex, multidisciplinary surgical therapy, with various sources of variability along the treatment pathway from target selection, intraoperative clinical patient testing, selection of electrode trajectory and site and surgical device placement to post-operative programming. A recent study reported that an inappropriate lead location was the most common cause for observed therapeutic failures (Pauls *et al.*, 2017). Indeed, more than half of motor outcome variability could be explained in our cohort by the anatomical distribution of stimulation, which is a combined effect of electrode location and stimulation parameters, particularly polarity settings, pulse duration and current amplitude.

Several previous studies have tried to identify the most effective site of electrode implantation or stimulation within the pallidal region. Tisch *et al.* (2007) found a more posterior electrode placement along the AC-PC axis, predictive

of better dystonia reduction in patients with generalized dystonia. Cheung *et al.* (2014) analysed a cohort of 21 dystonia patients carrying the *TOR1A* (*DYT1*) gene mutation, with excellent motor improvement using a more advanced approach, including VTA modelling; they also found the highest probability of benefit centred at the border between the middle and posterior third of the internal pallidum. An acute stimulation challenge in 20 cervical dystonia patients with stable, good motor response to DBS found the best acute response when stimulating near the lamina medullaris between the external and internal pallidum in the posterior and ventral segment of the two nuclei (Schonecker *et al.*, 2015). This region is also the source of theta oscillations, a potential biomarker of dystonia-associated network dysfunction (Neumann *et al.*, 2017), and maintains dense interconnections with premotor and primary cortical motor areas. Still, our heat map suggests that good outcomes can be achieved at different positions within the pallidal region. The ‘sweet spot’ volume is a result of statistical thresholding, which means it is the volume with highest probability of good outcome. Our prediction model, however, correctly identified patients with a predicted good outcome, whose VTAs did not overlap with the ‘sweet spot’ (Fig. 6, Case 3). How can these findings be explained in mechanistic terms? If one assumes that DBS acts by activating axons rather than cell bodies, the same

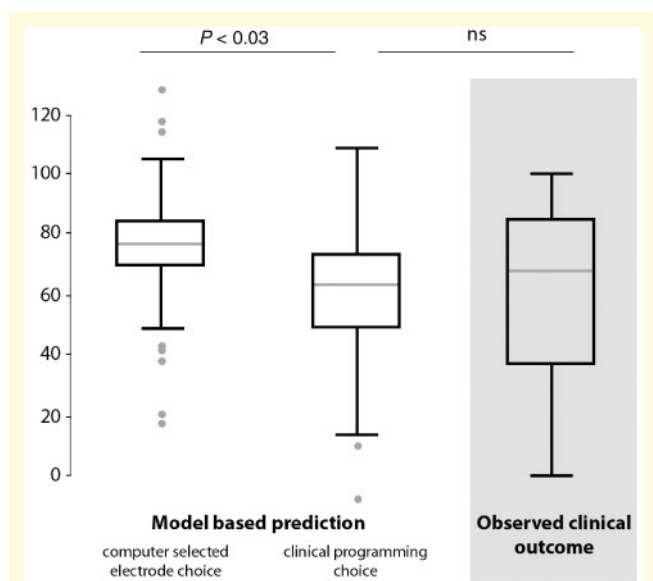


Figure 7 Exhaustive evaluation of all possible contact positions. Predicted dystonia improvement based on the VTA-atlas estimation model (left, middle) compared to the clinically observed outcome (right). *In silico* testing of all possible monopolar electrode choices with a predefined VTA (3.0 mA; 90 μ s) was used to determine the model based prediction of dystonia improvement for the ‘optimal’ computer selected electrode choice. Compared to clinically derived programming choices (middle) the predicted outcome is significantly higher ($60.5 \pm 21.9\%$ to $76.8 \pm 15.3\%$; $P < 0.03$). No differences between model based prediction of dystonia improvement for the clinical programming choices to observed clinical outcome (right).

fibre can be activated at many, even distant sites along its length; however, the most consistent benefit at a group level, would be observed at the anatomical sites where fibres converge into bundles. This hypothesis of better outcome with stimulation of white matter tracts fits well with increasing evidence from biophysical theory and experimental studies, that clinical effects of DBS are largely explained by ortho- or antidromic modulation of fibre pathway activity (Gunalan *et al.*, 2017). Moreover, stimulation volumes of ring electrodes at different spatial locations may overlap in critical volumes for optimal outcome. This may explain some divergence between outcomes of VTA and electrode mapping. Our findings emphasize that optimal outcomes of DBS would require a ‘volume planning’ rather than a ‘target point’ planning, which is the current standard in functional and stereotactic neurosurgery. This is particularly important in the light of directional leads and stimulation technologies such as multiple independent current control (MICC), which provide an unprecedented flexibility in the creation of a VTA with an implanted lead. In these cases, one can no longer assume a fixed spatial relation between VTA and contact location.

VTA modelling is a novel digital tool for estimating the volume of axon potential initiation by DBS (Butson *et al.*,

2011). Current VTA models account for certain stimulation parameters, tissue impedance and tissue anisotropy (McNeal, 1976; Butson *et al.*, 2006). A possible limitation of these models is the dependency on *a priori* assumptions about the membrane properties of the stimulated axons. However, it was recently shown that the VTA mirrored such neuronal properties as determined by clinical neurophysiological methods (i.e. chronaxies) (Reich *et al.*, 2015). Finally, the VTA assumes that the primary effect of DBS is related to activation of myelinated axons, which was corroborated by several studies (Holsheimer *et al.*, 2000; Paxinos and Mai, 2004; Groppa *et al.*, 2014). Lesion network mapping has recently shown to be useful to search or confirm treatment targets of DBS (Horn *et al.*, 2017; Joutsa *et al.*, 2018a). To link lesions in different locations associated with relief of tremor showed a common brain network centred in the motor thalamus, the primary target of DBS in essential tremor (Joutsa *et al.*, 2018b). Interestingly, the same group show positive connectivity to the cerebellum and negative connectivity to the somatosensory cortex, their lesion brain network results from 25 cervical dystonia cases conforming to our defined antidystonic sweet spot (Corp *et al.*, submitted for publication).

Predicting and guiding pallidal deep brain stimulation

The high predictive values of our heat map analysis (VTA-atlas estimation) foster its utility in planning and programming pallidal DBS in dystonia. The majority of dystonia patients have a delayed clinical response after initiating effective DBS (Kupsch *et al.*, 2011). In these situations, a model determining the overlap of an estimated individual VTA with our probabilistic outcome map could guide the selection of optimal stimulation settings. Moreover, the need for revision of an inappropriately placed lead could be anticipated, reducing the duration of rescue programming attempts.

In the current form our model is capable of evaluating the anti-dystonic quality of a stimulating volume, which is the combined result of electrode location and programming. A conversion into an expert system for guiding electrode implantation and programming is computationally complex, because it requires searching an exhaustive space of possible solutions if no *a priori* constraints are provided. Software for computer-assisted programming would need to simulate and automatically evaluate a wide range of possible VTAs for an implanted lead to find the optimal stimulation settings based on the probabilistic outcome maps. At a subsequent development stage, one could leave the constraints of a fixed lead location and simulate variations of lead locations, which could be useful for the planning of DBS implantations. Of relevance, a fully automatized DBS planning is not feasible in our opinion, because the neurosurgeon has to account for a number of safety features (e.g. vessels, eloquent areas)

during trajectory and target planning, which have an important bearing on global DBS outcomes but are not covered by our prediction model. Despite its limitations, our anatomical volume-based model explained a large amount of variance in motor outcome in our cohort, thereby reaching the prediction value of a recently published, connectivity-based model in subthalamic DBS for Parkinson's disease (Horn *et al.*, 2017). Interestingly, Horn and colleagues did not find further improvement of the model by adding stimulation volume information to the electrode location, probably owing to a lesser degree of lead placement variability in the much smaller subthalamic nucleus compared to the GPi. Whether additional individual structural or functional connectivity profiles will further increase the predictive value of our model for dystonia patients remains to be tested in future studies. Nevertheless, the clinical potential of the current method using the VTA-atlas estimation alone is illustrated by our simulation of *in silico* programming choices. It predicted 16.3% better group mean improvement with computer selected electrode choices compared to physician based programming and a reduced proportion of non-responders. These predictions need to be assessed in a prospective clinical trial, which is under preparation.

Limitations

Caution is required in interpreting the 'antidystonic sweet spot' volume illustrated in Fig. 4 as the optimal site for electrode implantation. The 'sweet spot volume' is the result of statistical thresholding of a probabilistic map covering a large volume of the pallidum and adjacent white matter. Good outcomes were observed with electrodes throughout this volume. In Fig. 6, we feature a patient with major benefit from DBS, who had VTAs located in both GPe without any coverage of the 'sweet spot volume' (Fig. 6, bottom row). Interestingly, our model also predicted this observed outcome truthfully, because it accounts for the entire 3D probability distribution and not only the statistically-thresholded sweet spot region. Another limitation of this study lies in the restriction to patients with isolated dystonia. For the purpose of this analysis and in contrast to the 'real world experience' of DBS for dystonia, we selected a cohort of patients with similar clinical presentation and presumed idiopathic or genetic aetiology of dystonia. We also excluded patients with presence of contractures and suspicious history of a conversion disorder. We are fully aware that this is not representative for the entire group of patients receiving pallidal DBS, but the primary aim of this study was to demonstrate the outcome variability related to the stimulation volume and therefore we had to reduce the impact of confounding variables, which on the other hand limits the generalizability of our results to other forms of dystonia. Finally, outcomes of DBS may also vary with the choice of temporal pulse patterns such as stimulation frequency, which is not taken into consideration by current VTA models. We assessed the

relation between stimulation frequency and outcome in our cohort, which was using stimulation frequencies between 30 and 200 Hz. At the last visit, 42 patients were stimulated with 130 Hz and 26 with a frequency of 180 Hz or higher, which had no bearing on outcome ($P = 0.87$). Neither did a linear regression analysis reveal any significant correlation between stimulation frequency and outcome ($P = 0.42$). Our observation here is in line with recent reports (Isaias *et al.*, 2009) and trials on low frequency stimulation in dystonia (Velez-Lago *et al.*, 2012).

Conclusion

Our study suggests that good motor outcomes of pallidal neurostimulation for isolated dystonia can be achieved at different electrode positions within the pallidal region including adjacent white matter by a choice of appropriate stimulation settings. The highest degree of overlap of stimulation volumes with excellent outcome covered the ventro-posterior GPi and subpallidal white matter tracts. Modelling of the individual volume of tissue activated informed by probabilistic outcome brain mapping may be developed into a clinically useful tool for computer-assisted DBS programming in the future.

Funding

This study was sponsored in part by the Interdisziplinäres Zentrum für Klinische Forschung (IZKF) of the University Hospital Wuerzburg (Grant number Z-2/64) and by an unrestricted research grant from Medtronic Inc., Minneapolis, MN, USA.

Competing interests

The authors report no competing interests.

Supplementary material

Supplementary material is available at *Brain* online.

References

- Albanese A, Bhatia K, Bressman SB, Delong MR, Fahn S, Fung VS, et al. Phenomenology and classification of dystonia: a consensus update. *Mov Disord* 2013; 28: 863–73.
- Andrews C, Aviles-Olmos I, Hariz M, Foltynic T. Which patients with dystonia benefit from deep brain stimulation? A meta-regression of individual patient outcomes. *J Neurol Neurosurg Psychiatry* 2010; 81: 1383–9.
- Arlot S, Celisse A. A survey of cross-validation procedures for model selection. *Statist Surv* 2010; 4: 40–79.
- Astrom M, Diczfalusy E, Martens H, Wardell K. Relationship between neural activation and electric field distribution during deep brain stimulation. *IEEE Trans Biomed Eng* 2015; 62: 664–72.

- Bruggemann N, Kuhn A, Schneider SA, Kamm C, Wolters A, Krause P, et al. Short- and long-term outcome of chronic pallidal neurostimulation in monogenic isolated dystonia. *Neurology* 2015; 84: 895–903.
- Butson CR, Cooper SE, Henderson JM, Wolgamuth B, McIntyre CC. Probabilistic analysis of activation volumes generated during deep brain stimulation. *Neuroimage* 2011; 54: 2096–104.
- Butson CR, Moks CB, McIntyre CC. Sources and effects of electrode impedance during deep brain stimulation. *Clin Neurophysiol* 2006; 117: 447–54.
- Cheung T, Noecker AM, Alterman RL, McIntyre CC, Tagliati M. Defining a therapeutic target for pallidal deep brain stimulation for dystonia. *Ann Neurol* 2014; 76: 22–30.
- Contarino MF, Smit M, van den Dool J, Volkmann J, Tijssen MA. Unmet needs in the management of cervical dystonia. *Front Neurol* 2016; 7: 165.
- Fonov VS, Evans AC, McKinstry RC, Almlí CR, Collins DL. Unbiased nonlinear average age-appropriate brain templates from birth to adulthood. *NeuroImage* 2009; 47: S102.
- Groppa S, Herzog J, Falk D, Riedel C, Deuschl G, Volkmann J. Physiological and anatomical decomposition of subthalamic neurostimulation effects in essential tremor. *Brain* 2014; 137 (Pt 1): 109–21.
- Gunalan K, Chaturvedi A, Howell B, Duchin Y, Lempka SF, Patriat R, et al. Creating and parameterizing patient-specific deep brain stimulation pathway-activation models using the hyperdirect pathway as an example. *PLoS One* 2017; 12: e0176132.
- Hamani C, Moro E, Zadikoff C, Poon YY, Lozano AM. Location of active contacts in patients with primary dystonia treated with globus pallidus deep brain stimulation. *Neurosurgery* 2008; 62 (3 Suppl 1): 217–23; discussion 23–5.
- Hemm S, Coste J, Gabrillargues J, Ouchchane L, Sarry L, Caire F, et al. Contact position analysis of deep brain stimulation electrodes on post-operative CT images. *Acta neurochirurgica* 2009; 151: 823–9; discussion 9.
- Holloway KL, Baron MS, Brown R, Cifu DX, Carne W, Ramakrishnan V. Deep brain stimulation for dystonia: a meta-analysis. *Neuromodulation* 2006; 9: 253–61.
- Holsheimer J, Demeulemeester H, Nuttin B, de Sutter P. Identification of the target neuronal elements in electrical deep brain stimulation. *Eur J Neurosci* 2000; 12: 4573–7.
- Horn A, Kuhn AA. Lead-DBS: a toolbox for deep brain stimulation electrode localizations and visualizations. *Neuroimage* 2015; 107: 127–35.
- Horn A, Reich M, Vorwerk J, Li N, Wenzel G, Fang Q, et al. Connectivity predicts deep brain stimulation outcome in Parkinson disease. *Ann Neurol* 2017; 82: 67–78.
- Isaias IU, Alterman RL, Tagliati M. Outcome predictors of pallidal stimulation in patients with primary dystonia: the role of disease duration. *Brain* 2008; 131 (Pt 7): 1895–902.
- Isaias IU, Alterman RL, Tagliati M. Deep brain stimulation for primary generalized dystonia: long-term outcomes. *Arch Neurol* 2009; 66: 465–70.
- Jinnah HA, Alterman R, Klein C, Krauss JK, Moro E, Vidailhet M, et al. Deep brain stimulation for dystonia: a novel perspective on the value of genetic testing. *J Neural Transm (Vienna)* 2017; 124: 417–30.
- Joutsa J, Horn A, Hsu J, Fox MD. Localizing Parkinsonism based on focal brain lesions. *Brain* 2018a.
- Joutsa J, Shih LC, Horn A, Reich MM, Wu O, Rost NS, et al. Identifying therapeutic targets from spontaneous beneficial brain lesions. *Ann Neurol* 2018b; 84: 153–7.
- Kupsch A, Benecke R, Müller J, Trottenberg T, Schneider GH, Poewe W, et al. Pallidal deep-brain stimulation in primary generalized or segmental dystonia. *N Engl J Med* 2006; 355: 1978–90.
- Kupsch A, Tagliati M, Vidailhet M, Aziz T, Krack P, Moro E, et al. Early postoperative management of DBS in dystonia: programming, response to stimulation, adverse events, medication changes, evaluations, and troubleshooting. *Mov Disord* 2011; 26 (Suppl 1): S37–53.
- McNeal DR. Analysis of a model for excitation of myelinated nerve. *IEEE Trans Biomed Eng* 1976; 23: 329–37.
- Neumann WJ, Horn A, Ewert S, Huebl J, Brücke C, Slentz C, et al. A localized pallidal physiologic marker in cervical dystonia. *Ann Neurol* 2017; 82: 912–24.
- Park HR, Lee JM, Ehm G, Yang HJ, Song IH, Lim YH, et al. Correlation of electrode position and clinical outcomes in globus pallidus stimulation for dystonia. *Acta Neurochir (Wien)* 2017; 159: 1349–55.
- Pauls KAM, Krauss JK, Kampfer CE, Kuhn AA, Schrader C, Sudmeyer M, et al. Causes of failure of pallidal deep brain stimulation in cases with pre-operative diagnosis of isolated dystonia. *Parkinsonism Relat Disord* 2017; 43: 38–48.
- Paxinos G, Mai Jk. The human nervous system. 2nd edn. Amsterdam; Boston: Elsevier Academic Press; 2004.
- Pollo C, Villemure JG, Vingerhoets F, Ghika J, Maeder P, Meuli R. Magnetic resonance artifact induced by the electrode Activa 3389: an in vitro and in vivo study. *Acta Neurochir (Wien)* 2004; 146: 161–4.
- Reich MM, Steigerwald F, Sawalhe AD, Reese R, Gunalan K, Johannes S, et al. Short pulse width widens the therapeutic window of subthalamic neurostimulation. *Ann Clin Transl Neurol* 2015; 2: 427–32.
- Schonecker T, Gruber D, Kivi A, Müller B, Lobsien E, Schneider GH, et al. Postoperative MRI localisation of electrodes and clinical efficacy of pallidal deep brain stimulation in cervical dystonia. *J Neurol Neurosurg Psychiatry* 2015; 86: 833–9.
- Tisch S, Zrinzo L, Limousin P, Bhatia KP, Quinn N, Ashkan K, et al. Effect of electrode contact location on clinical efficacy of pallidal deep brain stimulation in primary generalised dystonia. *J Neurol Neurosurg Psychiatry* 2007; 78: 1314–9.
- Trujillo-Ortiz A, Hernandez-Walls R, Castro-Perez A, Rodriguez-Cardozo L, Ramos-Delgado NA, Garcia-Sanchez R. Barnardtest: Barnard's exact probability test. A MATLAB file. 2004. <http://www.mathworks.com/matlabcentral/fileexchange/loadFile.do?objectId=6198>
- Vasques X, Cif L, Hess O, Gavarini S, Mennessier G, Coubes P. Prognostic value of globus pallidus internus volume in primary dystonia treated by deep brain stimulation. *J Neurosurg* 2009; 110: 220–8.
- Velez-Lago FM, Oyama G, Foote KD, Hwynn N, Zeilman P, Jacobson C, et al. Low-frequency deep brain stimulation for dystonia: lower is not always better. *Tremor Other Hyperkinet Mov (N Y)* 2012; 2: pii: tre-02-55-272-1. doi: 10.7916/D85X27PH.
- Vidailhet M, Vercueil L, Houeto JL, Krystkowiak P, Benabid AL, Cornu P, et al. Bilateral deep-brain stimulation of the globus pallidus in primary generalized dystonia. *N Engl J Med* 2005; 352: 459–67.
- Vidailhet M, Vercueil L, Houeto JL, Krystkowiak P, Lagrange C, Yelnik J, et al. Bilateral, pallidal, deep-brain stimulation in primary generalised dystonia: a prospective 3 year follow-up study. *Lancet Neurol* 2007; 6: 223–9.
- Volkmann J, Müller J, Deuschl G, Kuhn AA, Krauss JK, Poewe W, et al. Pallidal neurostimulation in patients with medication-refractory cervical dystonia: a randomised, sham-controlled trial. *Lancet Neurol* 2014; 13: 875–84.
- Volkmann J, Wolters A, Kupsch A, Müller J, Kuhn AA, Schneider GH, et al. Pallidal deep brain stimulation in patients with primary generalised or segmental dystonia: 5-year follow-up of a randomised trial. *Lancet Neurol* 2012; 11: 1029–38.
- Walsh RA, Sidiropoulos C, Lozano AM, Hodaie M, Poon YY, Fallis M, et al. Bilateral pallidal stimulation in cervical dystonia: blinded evidence of benefit beyond 5 years. *Brain* 2013; 136 (Pt 3): 761–9.
- Yelnik J, Bardin E, Dormont D, Malandain G, Ourselin S, Tande D, et al. A three-dimensional, histological and deformable atlas of the human basal ganglia. I. Atlas construction based on immunohistochemical and MRI data. *Neuroimage* 2007; 34: 618–38.